Engineered Nanomaterial Exposure Affects Organelle Genetic Material Replication in Arabidopsis thaliana

Engineered nanomaterial exposure controls organelle genetic material replication in Arabidopsis thaliana

Journal:	*ACS Nano*
Manuscript ID	Draft
Manuscript Type:	Article
Date Submitted by the Author:	n/a
Complete List of Authors:	Pagano, Luca; University of Parma, Chemistry, Life Science and Environmental Sustainability Marmiroli, Marta; Universita degli Studi di Parma, Dept. Environmental Sciences Villani, Marco; CNR, IMEM Magnani, Jacopo; University of Parma Rossi, Riccardo; University of Parma Zappettini, Andrea; CNR, IMEM White, Jason; Connecticut Agricultural Experiment Station, Department of Analytical Chemistry Marmiroli, Nelson; Universita degli Studi di Parma, Department of Chemistry, Life Sciences and Environmental Sustainability

Engineered nanomaterial exposure controls organelle genetic material replication in *Arabidopsis thaliana*

Luca Pagano,[1] Marta Marmiroli,[1,*] Marco Villani,[2] Jacopo Magnani,[1] Riccardo Rossi,[1] Andrea Zappettini,[2] Jason C. White,[3] Nelson Marmiroli[1,4]

[1] Department of Chemistry, Life Sciences and Environmental Sustainability, University of Parma, Parco Area delle Scienze 11/A, 43124 Parma, Italy.

[2] IMEM-CNR, Parco Area Delle Scienze 37/A, 43124 Parma, Italy.

[3] The Connecticut Agricultural Experiment Station, 123 Huntington Street, 06504 New Haven, CT, USA.

[4] Consorzio Interuniversitario Nazionale per le Scienze Ambientali (CINSA), University of Parma, 43124 Parma, Italy.

* marta.marmiroli@unipr.it. Phone: +39 0521 905698.

Abstract

Although a robust literature has been investigating biological effects of engineered nanomaterial exposure (ENMs) at cellular, tissue and organism levels, wide differences in experimental design confound a systemic analysis. Mitochondria and chloroplast are not only the cellular energy sources but also have important regulatory and developmental roles in cell function. CeO_2, FeOx ENMs, ZnS, CdS QDs and relative metal salts were utilized *in vitro* at different concentrations and times of exposures. Analysis of physiological and molecular response of *A. thaliana* chloroplast and mitochondrion demonstrates that ENMs modify functionality and organelle genome replication. Exposure to nanoscale CeO_2 and FeOx induced significant increase in biomass, whereas ZnS QDs and CdS QDs yielded neutral or negative effects on growth. Differential effects between ENMs and their corresponding metal salts highlight nanoscale-specific response pathways. Data from the different Fe forms suggest that the extent to which an ENM and its metal salt differ is a direct function

of ENM dissolution rate, toxicity of the metal ion released, and eventual biotransformation processes occurring within the plant. With regard to specific effects on ptDNA and mtDNA, CdS QD exposure triggered potential variations at sub-stoichiometric level in the two organellar genomes, while nanoscale FeOx and ZnS QDs caused an increase in ptDNA and mtDNA copy number. Nanoparticle CeO_2 exposure did not affect ptDNA and mtDNA stoichiometry. These findings suggest that modification in stoichiometry as potential morpho-functional adaptive response to ENMs exposure, triggered by modifications of bioenergetic redox balance which leads to reduce the photosynthesis or cellular respiration rate.

Keywords: nanomaterials, copy number variation, mitochondria, chloroplasts, *Arabidopsis thaliana.*

In the last decade, a wide range of engineered nanomaterials (ENMs) of different types have seen increasing use in industrial applications, consumer and medical products, and agriculture; application of these materials is projected to continue increasing.[1] Concerns over the environmental fate and effects of these materials have fostered studies to predict environmental concentrations in air, water, and soil, as well as efforts to determine threshold concentrations for eco-toxicological effects on terrestrial or aquatic biota.[2] Therefore, it is important to develop exposure biomarkers to the different types of nanoparticles that are potentially accumulating in the environment.[3] These assessments can be complicated by the nature of ENM use and release. For example, the occurrence of ENMs in agriculture can be through intentional means to achieve benefits after uptake by plants roots and foliage,[4,5] but also may occur incidentally through aerial deposition or presence in land applied biosolids.

A robust literature has developed in recent years evaluating plant interactions with ENMs, from both an application and implication perspective,[6] and the involvement of both the chloroplast and mitochondrion as key targets of ENMs response has become clear.[7,8,9] Plastids and mitochondria

are thought to have originated from independent endosymbiotic events,[10] wherein cyanobacteria-like and α-proteobacteria-like organisms became fully integrated with their host eukaryotic cells. Although mitochondria were likely derived from a single endosymbiotic event, plastids are thought to have evolved through multiple endosymbiotic events.[11] Although many genes moved from the organellar DNA to the "host" nucleus over evolutionary time, both plastids and mitochondria retain their own DNA that is unique in terms of architecture, size and content.[12,13] As the mitochondria and chloroplasts involve highly dynamic oxidation-reduction (RedOx) processes to support their bioenergetic activity, the organelle genomes may be particularly sensitive to mutational damage caused by excessive production of reactive oxygen species (ROS).[10] In addition, this organelle DNA lacks the protective protein scaffold found in nuclear DNA, and the overall higher replication rate make these genomes highly susceptible to mutation caused by a number of effectors (e.g. mutagens, stressors, environmental conditions).[10,14] Due to their structure of prokaryotic origin (a collection of linear, highly branched and occasionally circulars molecules), limited size, and high copy number per cell, the organellar genomes are subject to a physiological balance between fission/fusion processes and selective pressure dynamics that lead to a certain degree of heteroplasmic variance.[10,15] These recombinational phenomena are well known in the mitochondria of different organisms, from simple eukaryotes (e.g. *Saccharomyces cerevisiae*) to plants and humans.[10,12-14] In plastids, these mechanisms are recognizable, although their significance and their modes of action are still unclear.[16] Indeed, selective effectors like abiotic stress may cause organellar DNA damage and/or copy number variation, as reported for plastid DNA in *Arabidopsis thaliana* under salt stress.[17] In general, both the whole number of plastids and mitochondria and their full functionality constitute an indicator of plant health and as such, disturbance of these levels may hold a value as a biomarker of stress exposure.[8]

A number of ENMs present significant risk of exposure to plant materials. For example, nanoscale CeO_2 has been investigated as a novel nano-fertilizer, with effects varying as a function of both plant species and dose.[18,19] These applications have led to the frequent detection of CeO_2 ENMs in the environment, with agricultural soil being the predominant sink.[20] The impact of nanoscale

Fe_2O_3 and Fe_3O_4 on plants has been investigated by a number of groups, with variable results reported and overall impact often depending on the EMN form utilized: reduced chlorophyll production and biomass or improved root elongation.[21-23] For example, Kokina et al. (2017)[24] reported that Fe_3O_4 NPs did have beneficial effects on photosynthesis and growth. CdS QDs have exhibited toxicity to a number of species.[8,25,26]

The present study assessed the potential genetic effects of a range of engineered nanomaterials at different doses and exposure times. Importantly, measured endpoints included structural integrity and abundance of the organelle genetic information, both mitochondrial DNA (mtDNA) and plastid DNA (ptDNA). Two sets of experiments were conducted: the first focused on evaluating the responses of wild type *Arabidopsis thaliana* to CdS QDs, as well as corresponding metal salt, at different treatment times and concentrations. The second compared plant response to CdS QDs with the response to CeO_2, Fe_2O_3, Fe_3O_4 ENMs and ZnS QDs, as well as their corresponding metal salt forms. By evaluating the correlation between the physiological parameters associated with mitochondrial and chloroplast function with the organellar DNA copy number, we aimed to uncover the significance of organelle involvement in ENMs response and to demonstrate the potential utility of mtDNA and ptDNA copy number modulation as biomarker of exposure.

Results and Discussion

Replication of ptDNA and mtDNA during CdS QDs and $CdSO_4$ exposure

As shown in Figure 1 and Table S1, treatment of plants with CdS QDs and $CdSO_4$ resulted in different effects on ptDNA and mtDNA copy number and integrity, depending both on the exposure time and concentration. All data were normalized to the untreated control (T0 NT). In addition, some changes in ptDNA gene copy number are also evident in the controls T10 NT and T20 NT (*YCF1* and *PSBD*) (Figure 1c). Considering the T10 Cd(II) and T20 Cd(II) treatments with $CdSO_4$, it appears that the copy numbers were quite similar across all markers considered. The genes that showed a

significant copy number increase were *YCF1* and *PSBA*, while results obtained for *ORF31* (*PETL*) and *PSBF* (very close on the ptDNA map) were more similar to the untreated controls (T10 NT, T20 NT) (Figure 1c, Table S1). For the treatments (T10 QD 40, T10 QD 80, T20 QD 40 and T20 QD 80), the ptDNA gene copy number increased as observed for the $CdSO_4$ exposure. Similarity between the effect of nanoscale and ionic Cd treatments increased with the time of exposure. This can be explained by the time-dependent increase in ionic Cd after long exposure to CdS QDs, and specifically to the intracellular modification or biotransformation of CdS QD within the plant, as recently demonstrated in *Arabidopsis thaliana* by Marmiroli *et al.* (2020).[27] When considering each single target gene more closely, it is evident that the increase in ptDNA copy number was not generalized to the whole organellar genome. For example, *PSAC* and *YCF1*, located in the short single copy region (SSC), as well as *PSBA* and *PSBD*, located in long single copy region (LSC), all showed a consistent copy number across all the treatments. Conversely, *ORF31* and *PSBF* showed a general similarity to the untreated control in nearly all conditions, with the exception of T10 QD 40 (Figure 1c). This phenomenon suggests a potential sub-stoichiometric shifting of the ptDNA, according to the definition of Woloszynska & Trojanowski (2009),[15] has been previously observed during plant development or stress response.[10,17,28] This can be considered a dynamic process by which the organellar DNA copy number (or DNA fragments) may undergo changes over the course of a single generation. Sub-stoichiometric shift was proposed as result of recombination increased frequency or selective replication of DNA fragments, which may also occur by selective transmission of DNA molecules during organelle division.[15] Interestingly, several ptDNA markers, including *ORF31,* are co-expressed with the gene *ZAT12*, which encodes for a transcription factor involved in abiotic stress response, and plays a key role in ROS signaling pathway.[29] Treatment with CdS QDs at 150-250 mg L^{-1} produced effects more similar to the untreated controls with regard to ptDNA gene copy numbers. Since the growth inhibition concentration was previously estimated at 130 mg L^{-1},[30] this response is suggestive of complete inhibition of the organelle functions, which results in the maintenance of the ptDNA copy number during this high level of stress or during plant senescence.[10]

The mtDNA analyses (Figure 1d, Table S1) had some similarity to those of ptDNA for the $CdSO_4$ treatments (T10 Cd(II), T20 Cd(II) treatments). Specifically, mtDNA showed that for *COX1* and *COB*, the gene copy number was increased in several treatments (T10 QD 80, T20 Cd(II) 50, T20 Cd(II) 100), whereas *CCB206*, *CCB256* and *CCB382* remained largely unchanged. These findings may suggest a potential mtDNA reorganization after exposure. It remains uncertain whether the observed effects on mtDNA were due to replication or recombination (or both), and if they derived directly from the Cd^{2+} ion, considering its known genotoxic effects on nucleic acids,[31] or from the stress-induced production of ROS related to CdS QDs interaction with the inner mitochondrial structures.[8,26,32] Similar to what observed in ptDNA, the amplification of several mtDNA markers has been associated with response to abiotic stress conditions, such as cold or drought.[33] Interestingly, by comparing gene copy number and gene expression of the target genes (Figure S1 and Table S2), it is possible to observe a correlation between stoichiometric modification of the organellar DNA and the relative expression of the same mitochondrial genes.

Effect on organellar DNA during ENMs exposure

Analyses of gene copy number for ptDNA highlights some important features. The heatmaps (Figure 1e, Table S1) show that for $FeCl_3$, $ZnSO_4$, ZnS QDs, Fe_3O_4 ENMs treatments, the copy number of the six target genes was uniformly increased, whereas a negligible effect was observed upon exposure to Fe_2O_3 NPs, CeO_2 NPs and $CeCl_3$ as compared with the untreated control. In all cases, it is clear that the amplification phenomenon may involve all markers along the entire ptDNA sequence, whereas for CdS QDs or $CdSO_4$ treatments, the amplification was specific only to certain markers of ptDNA (Figure 1c, Table S1). A chord diagram was constructed (Figure 2a) to clarify the relationships between the different amplification phenomena that occurred during treatment, in terms of differences and commonalities. For example, Fe- and Zn-based treatments produced a significant overlap, with all gene targets that increase in copy number ranging between 1 to 3-fold. For Cd-based treatments, there were differential trends in amplification of the targets: increases of *YCF1* or *PSAC*,

PSBA; decreases of *ORF31*, *PSBF*), whereas for Ce-based materials, there were no significant changes as compared to the control.

The presence of a specific metal in the treatment, as nanoscale or ionic form, determined the differences and similarities in the responses. For example, in the Ce-based treatments (both as ionic or nanoscale), the copy number was similar to the untreated controls, whereas for the Zn-based treatments, there was an increase in ptDNA copy number. Treatment with different Fe-based compounds showed an increase in ptDNA gene copy number with the order: Fe_2O_3 ENMs < Fe_3O_4 ENMs < $FeCl_3$. A potential explanation may be related to the differential stability of the three forms of Fe (Tables 1, 2). While the $FeCl_3$ salt has a theoretical value of dissolution (in ddH_2O) of 100%, the Fe_2O_3 and Fe_3O_4 ENMs showed a much lower percentage of dissolution (Table 1), suggesting a correlation between ptDNA amplification and with ROS generation by Fe ion presence,[17,34,35] and with the modulation of the cellular redox state.[10,28,36] $ZnSO_4$ and ZnS QDs treatments caused a significant amplification in ptDNA markers; this effect could be partially attributed to released Zn ions, but this does not explain the entirety of the effects with ZnS QDs, whose dissolution is limited in ddH_2O (Table 1). This may suggest, as for CdS QDs, that in planta biotransformation processes were responsible for the generation of active Zn or Cd forms within the tissues that in turn promoted ptDNA amplification. [27]

A similar trend in target gene amplification was observed for mtDNA (Figures 1f, 2b; Table S1). Specifically, $FeCl_3$, $ZnSO_4$, ZnS QDs, and Fe_3O_4 ENMs treatments caused a significant increase in copy number, with values in the range of 1 to 3-fold for all the target genes analyzed. Conversely, exposure to Fe_2O_3 ENMs, CeO_2 ENMs and $CeCl_3$ decreased or had no effect on copy number. Treatment with $CdSO_4$ and CdS QDs induced a different response, causing a 2-fold decrease in copy number for the target genes *CCB382* and *CCB206*. Comparison between the amplification profiles of ptDNA and mtDNA suggests that for these treatments, a general uniform response was evident for both organelles with regard to DNA replication.

Effects of ENMs treatments on plant physiology

The results of the physiological analyses from plants exposed to the ENMs and the corresponding metal salts are reported in Figure 3 and Tables S3-S5. Treatment with Fe_2O_3, Fe_3O_4 and CeO_2 ENMs doubled the total biomass, as compared to the untreated control (Figures 3, S2; Table S3). Conversely, a decrease in biomass was evident after exposure to the four metal salts ($CeCl_3$, $FeCl_3$, $ZnSO_4$ and $CdSO_4$) and to CdS QDs (Figure 3). ZnS QDs treatment had no effect on biomass, with results equivalent to the untreated control. Normalizing the biomass parameter of the treated samples to the control value allowed to distinguish three effects on biomass: positive, neutral and negative (Figure S2). With regard to photosynthetic efficiency (Table S4), Fe_3O_4 NPs exposure caused a marked increase in chlorophyll *a* and *b* accumulation, respectively; 1.852 ± 0.636 and 0.767 ± 0.197, as compared with the control values of 0.989 ± 0.367 and 0.535 ± 0.271, respectively. Plants treated with $CdSO_4$ showed a significant decrease in chlorophyll *a*, and exposure to $CeCl_3$, $ZnSO_4$, ZnS QDs, $CdSO_4$, CdS QDs significantly decreased chlorophyll *b* production. No significant differences were observed in carotenoid levels of the treatments, because this class of pigments is rapidly deployed to quench the initial ROS burst likely induced by exposure.[26] For CdS QDs, the results were consistent with previous studies of exposure at different concentrations and exposure times,[26] where the biomass, and photosynthetic pigments were significantly decreased. Analyzing the results from the plant cell respiration (TTC assay, Table S5), exposure to Fe_2O_3, Fe_3O_4 and CeO_2 ENMs treatments significantly increased respiration, suggesting adequate mitochondrial functionality and aligning with the positive effects on plant biomass. Conversely $CdSO_4$ and CdS QDs treatments showed a decrease in respiration, suggesting an inhibition of mitochondrial function. These findings are also consistent with the observed biomass reductions for these treatments.[8,26]

The effects of nanoscale Fe_2O_3, Fe_3O_4 and CeO_2 treatments differed from those obtained with corresponding ionic forms. Concerning CeO_2 NPs and $CeCl_3$, the results obtained fit with reports for *Arabidopsis thaliana*[37] and other crops species.[3,9,18,38] Nanoscale CeO_2 stimulates vegetative growth; the effect being related to the antioxidant properties of co-existing Ce^{4+} and Ce^{3+} valence forms.[39,40]

For the iron oxide-based ENMs (Fe_2O_3, Fe_3O_4), the results are also in keeping with the current literature, where positive or neutral effects on the vegetative growth of *Arabidopsis thaliana* and *Triticum aestivum* L.[24,41] have been reported, but also with negative effects on biomass during $FeCl_3$ exposure.[42] With regard to CdS QDs and $CdSO_4$, the negative effects on biomass and other physiological parameters were also consistent with previous studies[26,30] as with a strong decrease in photosynthetic activity and cellular respiration as a consequence of disrupted organellar functions with increasing exposure time and CdS QDs concentration.[8] It has been demonstrated that CdS QDs and $CdSO_4$ trigger different regulatory responses at the level of mRNA and proteins.[25,27,30,37,43] Concerning the effects observed for ZnS QDs, the literature related to this pristine type of QD is minimal. However, information related to ZnO NPs effects on plant species is abundant,[9] and mostly in agreement with the results reported in Ruotolo *et al.* (2018):[37] decreased chlorophyll production and induction of secondary metabolite biosynthesis.

Analysis of physiological and molecular components of ENM and ionic response

A Principal Component Analysis (PCA) based model was constructed for both the mitochondria and chloroplasts to provide a mechanistic interpretation of each organelle involvement in response to ionic and nanoscale metal exposure and to explain the positive, neutral and negative effects on ptDNA and mtDNA replication and that plant physiological effects (Figure 4). The observed effects depend mainly on i) the elemental composition of the ENM, ii) whether the form was nanoscale or ionic, iii) the physico-chemical stability of the ENM in water, as compared with salt taken as reference. The parameters considered for this analysis were: biomass index (Figure S2), ptDNA and mtDNA copy number variation (Figure 1), photosynthetic activity (Table S4) and cellular respiration (Table S5). Analyzing the two major components based on the total variance revealed that for the chloroplast and mitochondrion, a similar correlation was observed, not only demonstrating how the effects were common to both organelles but also that the overall organellar function was deterministic of the overall plant phenotypic response under stress conditions.[14,44] For the chloroplast,

the first two components represent 51.6% and 34.7% of the total variance (Figure 4a), whereas for mitochondrion, the first two components represent the 63.2% and 33.5% of the total variance (Figure 4b). In both cases, the first component was determined by the type and form of the compound used (nanoscale or ionic form), as shown by the different effects between nanoscale FeOx or CeOx-based treatments and their associated ionic forms in terms of biomass index. Conversely, for CdS QD and ZnS QD treatments, the response was similar to that obtained with the respective ionic forms. In the case of ZnS QDs, it should be considered that the release of Zn^{2+} ions is higher than Cd^{2+} from CdS QDs, at least when considering dissolution in water (Tables 1, 2). However, ZnS QDs dissolution does not completely explain the observed results, suggesting that biotransformation phenomena may occur within the plant tissues and organs after ZnS QDs uptake. Indeed, for CdS QDs Marmiroli *et al*. (2020)[27] recently demonstrated that particle biotransformation can occur within the plant cell, resulting in a chemical form that is not consistent with ionic Cd. This difference between ionic and nanoscale form has been also demonstrated through unique genetic responses to CdS QDs and Cd^{2+} exposure,[8,30] and by a nanoscale specific proteomic response.[43]

The second component (Figure 4a) is related to the ptDNA and mtDNA copy number, separating the treatments that triggered a copy number increase (Fe_3O_4 NPs, $FeCl_3$, ZnS QDs, $ZnSO_4$) from those that had no effect ($CeCl_3$, CeO_2 NPs, Fe_2O_3 NPs) or those that had a non-uniform impact on ptDNA and mtDNA (CdS QDs, $CdSO_4$). With the Ce-based treatments, the effects observed on the biomass were different (Figure 3; Table S3), whereas the effects on ptDNA and mtDNA copy number were uniformly non-significant (Figure 1). These results are consistent with the fact that CeO_2 ENMs did not interfere with the functionality of either organelle, but did promote a ROS scavenging activity within the plant cell.[39,40] Conversely, $CeCl_3$ decreased the biomass production, as observed also in other plant species.[3] Interestingly, the Fe-based treatments decreased mitochondrial and chloroplast function (Figure 3, Tables S4, S5), but not the biomass index (Figure S2), and these materials caused an increase in ptDNA and mtDNA copy number. As noted above, this phenomenon is likely a function of the increase in $Fe^{2+/3+}$ concentration within the plant cell from $FeCl_3$ and,

partially, from FeOx (Table 1). Ionic Fe can increase ROS production through Fenton reactions that may trigger a stoichiometric increase in ptDNA and mtDNA in order to balance the physiological need of organelle function.[10,14,28,36,45]

In analyzing the physiological effects of exposure, it is clear that ptDNA and mtDNA copy number increased when biomass and photosynthesis activity or cellular respiration decreased. This may be an evidence of an interplay between the morpho-functional integration of the organelles and their replication/recombination machinery.[10,46,47] Upon exposure to an external stress, mtDNA and ptDNA were able to alleviate and accommodate the functional damage by modulating the copy number of some of their essential genes (Figure 1, Table S1). Evidence of this relationship can also be found at the gene expression level (Figure S1, Table S2), suggesting a role in response and adaptation to a broad range of different stressors.[29,33] Another consideration is that the oxidative stress generated by some ENMs or equivalent salts could also be an effector of the response at the systemic level, including functional modifications in the regulation of chloroplast and mitochondrial DNA replication.[7,8] This mechanism may be peculiar for organellar genomes and for their ability to adjust gene expression levels during stress conditions.

Conclusions

The primary finding of significance in this study is that organellar DNA molecules may change drastically in copy number during exposure to select metals in either nanoscale or ionic form. These nucleic acid effects may or may not be correlated with overt physiological changes in the plants. Importantly, the different physiological effects between ENMs and their corresponding metal salts highlight nanoscale-specific response pathways. These size-specific changes may rest upon differential metal availability from the salt or nanoscale forms, from the inherent metal toxicity (Cd>Zn>Fe>Ce), and from biotransformation processes that impact the material in the plant.[27] CdS QDs and $CdSO_4$ show the greatest potential to modify both ptDNA and mtDNA copy number, whereas CeO_2 NPs does not affect organellar DNAs. The results suggest that the effect on organellar

DNA replication is a plant adaptive response to the stress imposed by metal exposure and to the subsequent ROS production at organellar level.[10-14] A similar phenomenon was described for organellar DNAs in developing plants.[12,48] With recent experimental evidence, the conventional idea of organellar DNAs as exclusively closed loops have been updated with the idea that organellar DNA contains both linear and circular molecules.[12] During stress conditions, organellar proteins involved in DNA repair/replication, persist at similar expression levels by increasing the copy number of specific genes, as occurs for organellar ribosomes components.[49] This type of regulation appears increasingly relevant when considering all the cases of DNA abandonment where selected copies of organellar DNA (exclusively) are degraded because of damage accumulated during replication under conditions of stress.[50] Molecular integrity can change drastically during exposure to some metals in ionic and nanoscale forms as a consequence of inhibition of respiration and photosynthesis, as well as from activation of photorespiration and ROS production.[10,14] Disturbance at the organelle level produces a retrograde hormone signaling, likely modulated by ROS.[51] This may impact nuclear gene expression related to growth and development, as well as abiotic stress response. Abandonment of larger (unrepaired) organellar DNA molecules in this condition and replication of smaller circular DNAs in the organelles effectively block lesion transmission and modulate the availability of some organellar genes to the existing treatment stress (Figure 5). Interestingly, the same nanoscale or ionic responses were observed both for ptDNA and mtDNA. An explanation can be coordination to produce dual localized protein complexes involved in DNA replication/repair that are targeted to both chloroplast and mitochondria.[48,52] In this way, mitochondria and plastids respond similarly to stimuli such as metal stress, which change the redox state of the cell. When the need for protein involved in repair and replication is increased, the production of additional DNA able to restore organellar functionality is also increased.[10,12,14]

This study highlights the important relationship between ptDNA and mtDNA replication and organelle function, and serves as further evidence of the significant role of chloroplast and mitochondria in mediating plant response and adaptation to stress induced by exposure to metals in

nanoscale or salt forms. As such, changes in the copy number of ptDNA and mtDNA may be considered a putative biomarker of metal exposure (in both nanoscale or ionic form) in higher eukaryotes. This tool could be used when assessing potential exposure to ENMs, as well as for the monitoring of ENM presence and transfer through different environmental compartments.

Experimental section

ENMs characterization

CdS quantum dots (QDs), ZnS QDs, Fe_2O_3 NPs, and Fe_3O_4 NPs were synthesized by IMEM-CNR (Parma, Italy). CeO_2 NPs were purchased from Sigma-Aldrich (Merck, Darmstadt, Germany). All ENMs were characterized by X-ray diffraction (XRD) and transmission electron microscopy (TEM, Talos F200S G2, SEM FEG Thermo Fisher Scientific, Waltham, MA, USA). Additional information on ENM synthesis is reported in the Supporting Information (SI). The average particle size (*dh*) and zeta (ζ) potential of the ENMs (100 mg L^{-1}) were determined in ddH_2O on a Zetasizer Nano Series ZS90 (Malvern Instruments, Malvern, UK). ENM dissolution was investigated by ultracentrifugation ENMs standards (100 mg L^{-1}) prepared in ddH_2O after 20 days at 30000 rpm, 10 min, 20°C (Optima Max-XP Ultracentrifuge, Beckman-Coulter Inc., Brea, CA, USA). A 1 ml aliquot of the resulting solutions was digested in 4 mL of 1M HNO_3 for 20 min at 200°C using a VELP DK20 digester (VELP Scientifica, Usmate, Italy). The digests were analyzed by flame atomic absorption spectroscopy (FA-AAS) (AA240FS, Agilent Technologies, Santa Clara, CA, USA). ENM characterization and dissolution data are reported in Table 1, Figure 6 and Figures S3-S7.

Plant treatments

Wild type *Arabidopsis thaliana* (L.) Heynh, ecotype Landsberg erecta (Ler-0) was grown on a Murashige and Skoog (MS) medium (Duchefa Biochemie, Haarlem, The Netherlands) containing 1% w/v sucrose, 0.8% w/v agar, at 24°C. Plants were grown under 30% relative humidity with a 16

h photoperiod (light intensity 120 μM m^{-2} s^{-1} photosynthetic photon flux). After 10d of growth on non-treated MS medium, the seedlings were transferred to MS medium amended with the individual ENMs at a range of concentrations for different exposure periods as reported in Table 2. The ENMs were probe sonicated by a Fisher Scientific Model 505 Sonic Dismembrator (Fisher Scientific, Waltham, MA) at 40% amplitude for 60s to maximize dispersion before addition to the MS medium. The respective salts were included as controls. All the treatments were conducted with ten biological replicates.

Real Time qPCR on mtDNA and ptDNA

DNA extraction was performed from the whole plant tissues using the 2x CTAB protocol.[53] The copy number for mtDNA and ptDNA selected markers (Figure 1; Table S6) was determined by Real Time quantitative PCR (qPCR) using Applied Biosystems Power SYBR Green Master Mix chemistry (Applied Biosystems, Foster City, CA, USA) in an optical 96-well plate with the Applied Biosystems ABI PRISM 7900HT Sequence Detection System. Specific primers for each selected target were designed (Table S6) using the Primer3 software (primer3.ut.ee). Target genes were chosen on the basis of their position on the mtDNA and ptDNA biomolecules, so as to effectively characterize the organellar DNA sequences (Figure 1a, b).[10] Amplification followed the thermal profile: 95°C for 10', 95°C for 15" and 60°C for 60" (for 40 cycles). Synthesized primers (Sigma-Aldrich, St. Louis, MO, USA) were assessed by qPCR in four serial dilutions (1, 1:10, 1:100, 1:1000). Amplicons were confirmed by size and sequencing, performed by BMR Genomics service (Padova, ITA). Alignments were performed by BLAST tools (blast.ncbi.nlm.nih.gov/Blast.cgi). The relative quantity of DNA was estimated through the ΔΔCt method, using *rrn16* (encoding rRNA16) as reference gene. The relative quantity of each DNA sample was determined by normalization using the reference gene number of copies, and the arithmetic mean was calculated for three independent repeated reactions.

Physiological Parameters

Several physiological parameters were analyzed after plant harvest: fresh biomass, photosynthetic activity, and cellular respiration were determined according to the protocols below. The biomass index was calculated as the ratio between the fresh weight biomass values of each different treatments versus the untreated control. Photosynthetic pigment content was evaluated according to Ni *et al.*, (2009)[54] in order to assess photosynthetic activity. Briefly, portions of leaves (200 mg) were suspended in 800 μL 95% acetone. After incubation for 10 min on ice, the samples were centrifuged at 3000g and 4°C for 10 min, and chlorophyll *a*, chlorophyll *b*, and total carotenoids were determined by spectrophotometric analysis (Varian Cary 50, Agilent Technologies, Santa Clara, CA, USA) at 662 nm, 647 nm, 480 nm, respectively. The TTC (2,3,5-triphenyltetrazolium chloride) reduction assay was used as a quantitative method to assess the plant cell viability through respiration activity.[55] A 200 mg aliquot of fresh tissue was added to 3 mL of TTC buffer (TTC 0.18 M, 78% Na_2HPO_4 0.05 M, 22% KH_2PO_4 0.05 M). Samples were incubated at 30°C for 15h. Formazan, which results from TTC reduction, was extracted in 10 ml of 95% ethanol for 10 min at 80°C and was quantified spectrophotometrically at 530 nm (Varian Cary 50, Agilent Technologies, USA).

Statistics and bioinformatic analysis

Physiological parameters were evaluated by a one-way ANOVA with a pairwise Tukey's multiple comparison test (IBM SPSS v. 26.0). A two-tail Student *t* test was also applied to qPCR results. Chord diagram multiple comparisons were constructed through the Circos table viewer tool (http://mkweb.bcgsc.ca/tableviewer/). The R software (https://www.r-project.org/) was used for gene clustering and principal component analysis (PCA) of different treatments.

Author contributions

NM, MM, with contribution of JCW and LP supervised the project and designed all the experiments. LP, JM and RR performed the experiments with the contribution of MM. MV and AZ provided the FeOx ENMs, CdS QDs and ZnS QDs. All authors contributed and approved the final

manuscript.

Acknowledgements

The authors acknowledge Caterina Agrimonti, Silvia Carlo and Francesco Mezzadri from the Dept. of Chemistry, Life Science and Environmental Sustainability, for contributing to the molecular data analysis and for assistance in XRD analysis. LP acknowledges the support of FIL ("Fondi Locali per la Ricerca") 2018. MM, MV and AZ acknowledge the COMP-HUB Initiative, funded by the 'Departments of Excellence' program of the Italian Ministry for Education, University and Research (MIUR, 2018-2022). JCW acknowledges USDA NIFA CONH00147.

Notes

The authors declare no competing financial interest.

Supporting Information (SI)

Supporting information (SI) contain methods related to ENMs synthesis and characterization, sequence alignments and total RNA extraction with relative comparison to DNA amplification. Figure S1: schematic representation of the dissolution protocol. Figure S2: Biomass Index representation. Figures S3-S6: ENMs characterization by XRD; Figure S7: CdS QDs treatments comparison (gene copy number vs gene expression); Tables S1-S2: data from heatmaps (included in Figures 1, S1); Tables S3-S5: physiological parameters measurements and statistics; Table S6: primers sequences utilized in qPCR analyses.

References

1. Lv, J.; Christie, P.; Zhang, S. Uptake, translocation, and transformation of metal-based nanoparticles in plants: recent advances and methodological challenges. *Environ. Sci.: Nano*, **2019**, 6, 41-59.
2. Zhang, P.; Guo, Z.; Zhang, Z.; Fu, H.; White, J.C.; Lynch, I. Nanomaterial transformation in plants: Implications for food safety and application in agriculture. *Small*, **2020**, 16, 1-13. Doi: 10.1002/smll.202000705.
3. Pagano, L.; Servin, A.D.; De La Torre-Roche, R.; Mukherjee, A.; Majumdar, S.; Hawthorne, J.; Marmiroli, M.; Maestri, E.; Marra, R.E.; Isch, S.M.; et al. Molecular response of crop plants to engineered nanomaterials. *Environ. Sci. Technol*. **2016**, 50 (13), 7198−7207.
4. Kah, M.; Tufenkji, N.; White, J.C. Nano-enabled strategies to enhance crop nutrition and protection. *Nature Nanotechnology*, **2019**, 14, 532–540.
5. Hofmann, T.; Lowry, G.; Ghoshal, S.; Tufenkji, N.; Brambilla, D.; Dutcher, J.; Gilbertson, L.; Giraldo, J.P.; Kinsella, M.; del Capio Landry, M.; et al. Moving forward responsibly in nanotechnology enabled plant agriculture. *Nature Food,* **2020**, 1, 416–425.
6. Su, Y.; Ashworth, V.; Kim, C.; Adeleye, A.S.; Rolshausen, P.; Roper, C.; White, J.C.; Jassby, D. Delivery, uptake, fate, and transport of engineered nanoparticles in plants: A critical review and data analysis. Environ. Sci.: Nano. **2019**, 6, 2311-2331, DOI: 10.1039/C9EN00461K
7. Wang, Z.; Xu, L.; Zhao, J.; Wang, X.; White, J.C.; Xing, B. CuO Nanoparticle interaction with *Arabidopsis thaliana*: toxicity, parent- progeny transfer and gene expression. *Environ. Sci. Technol*., **2016**, 50, 6008.
8. Pagano, L.; Maestri, E.; Caldara, M.; White, J.C.; Marmiroli, N.; Marmiroli, M. Engineered nanomaterial activity at the organelle level: Impacts on the chloroplasts and mitochondria. *ACS Sustain. Chem. Eng*. **2018**, 6, 12562-12579.
9. Ma, C.; White, J.C.; Zhao, J.; Zhao, Q.; Xing, B. Uptake of Engineered Nanoparticles by Food

Crops: Characterization, Mechanisms, and Implications. *Annu. Rev. Food Sci. Technol*. **2018**, 9, 129–53.

10. Johnston, I.G. Tension and resolution: dynamic, evolving populations of organelle genomes within plant cells. *Mol. Plant*., **2019**, 12, 764-783.
11. Archibald, J.M. Endosymbiosis and Eukaryotic Cell Evolution. *Curr Biol.* **2015**, 25, 911-921.
12. Oldenburg, D.J.; Bendich, A.J. DNA maintenance in plastids and mitochondria of plants. *Front. Plant Sci.* **2015**, 6, 883. Doi: 10.3389/fpls.2015.00883.
13. Smith, D.R.; Keeling, P.J. Mitochondrial and plastid genome architecture: Reoccurring themes, but significant differences at the extremes. *PNAS*, **2015**, 112 (33), 10177-10184.
14. Zhao, L.; Sumberaz, P. Mitochondrial DNA Damage: Prevalence, Biological Consequence, and Emerging Pathways. *Chem. Res. Toxicol*. **2020**. Doi: 10.1021/acs.chemrestox.0c00083.
15. Woloszynska, M.; Trojanowski, D. Counting mtDNA molecules in *Phaseolus vulgaris*: sublimons are constantly produced by recombination via short repeats and undergo rigorous selection during substoichiometric shifting. *Plant Mol Biol*. **2009**, 70, 511-521.
16. Ruhlman, T.A.; Zhang, J.; Blazier, J.C.; Sabir, J.S.M.; Jansen, R.K. Recombination-dependent replication and gene conversion homogenize repeat sequences and diversify plastid genome structure. *Am. J. Bot*. **2017**, 104:559–572.
17. Peharec-Štefanić, P.; Koffler, T.; Adler, G.; Bar-Zvi, D. Chloroplasts of salt-grown arabidopsis seedlings are impaired in structure, genome copy number and transcript levels. *PLoS ONE*, **2013**, 8(12), 82548.
18. Cao, Z.; Rossi, L.; Stowers, C.; Zhang, W.; Lombardini, L.; Ma, X. The impact of cerium oxide nanoparticles on the physiology of soybean (Glycine max (L.) Merr.) under different soil moisture conditions. *Environ. Sci. Pollut. Res*. **2018**, 25, 930−939.
19. Zulfiqar, F.; Navarro, M.; Ashraf, M.; Akram, N.A.; Munné-Bosch, S. Nanofertilizer use for sustainable agriculture: Advantages and limitations. *Plant Science*, **2019**, 289, 110270.
20. Rossi, L.; Zhang, W.; Schwab, A.P.; Ma, X. Uptake, Accumulation, and in planta distribution

of coexisting cerium oxide nanoparticles and cadmium in *Glycine max* (L.) Merr. *Environ. Sci. Technol.* **2017**, 51, 12815-12824.

21. Hu, J.; Guo, H.; Li, J.; Gan, O.; Wang, Y.; Xing, B. Comparative impacts of iron oxide nanoparticles and ferric ions on the growth of *Citrus maxima*. *Environ Pollut.*, **2017**, 221, 199-208.
22. Zuverza-Mena, N.; Martínez-Fernández, D.; Du, W.; Hernandez-Viezcas, J.A.; Bonilla-Bird, N.; López-Moreno, M.L.; Komárek, M.; Peralta-Videa, J.R.; Gardea-Torresdey, J.L. Exposure of engineered nanomaterials to plants: Insights into the physiological and biochemical responses-A review. *Plant Physiol. Biochem*. **2017**, 110, 236−264.
23. Wang, A.; Jin, Q.; Miao, A.; White, J.C.; Gardea-Torresey, J.L.; Ji, R.; Zhao, L. High-throughput screening for engineered nanoparticles that enhance photosynthesis using mesophyll protoplasts. J. Agric. Food Chem. 2020. 68, 11, 3382-3389.
24. Kokina, I.; Mickevica, I.; Jahundovica, I.; Ogurcovs, A.; Krasovska, M.; Sonoka, M.J.; Mihailova, I.; Tamanis, E.; Gerbreders, V. Plant explants grown on medium supplemented with Fe3O4 nanoparticles have a significant increase in embryogenesis. *J. Nanomaterials*. **2017**, 4587147.
25. Majumdar, S.; Pagano, L.; Wohlschlegel, J.A.; Villani, M.; Zappettini, A.; White, J.C.; Keller, A.A. Proteomic, gene and metabolite characterization reveal the uptake and toxicity mechanisms of cadmium sulfide quantum dots in soybean plants. *Environ. Sci.: Nano*, **2019**, 6, 3010-3026.
26. Marmiroli, M.; Mussi, F.; Pagano, L.; Imperiale, D.; Lencioni, G.; Villani, M.; Zappettini, A.; White, J.C.; Marmiroli, N. Cadmium sulfide quantum dots impact *Arabidopsis thaliana* physiology and morphology. *Chemosphere*, **2020**, 240, 124856.
27. Marmiroli, M.; Lepore, G.O.; Pagano, L.; d'Acapito, F.; Gianoncelli, A.; Villani, M.;

Lazzarini, L.; White, J.C.; Marmiroli, N. The fate of CdS Quantum Dots in plants as revealed by Extended X-ray Absorption Fine Structure (EXAFS) analysis. *Environ. Sci.: Nano*, **2020**. Doi: 10.1039/C9EN01433K.

28. Kabeya, Y.; Miyagishima, S. Chloroplast DNA replication is regulated by the redox state independently of chloroplast division in *Chlamydomonas reinhardtii*. *Plant Physiology*, **2013**, 161, 2102–2112.
29. Davletova, S.; Schlauch, K.; Coutu, J.; Mittler, R. The zincfinger protein *Zat12* plays a central role in reactive oxygen and abiotic stress signaling in Arabidopsis. *Plant Physiol*. **2005**, 139, 847−856.
30. Marmiroli, M.; Pagano, L.; Savo Sardaro, M.L.; Villani, M.; Marmiroli, N. Genome-wide approach in *Arabidopsis thaliana* to assess the toxicity of cadmium sulfide quantum dots. *Environ. Sci. Technol*. **2014**, 48, 5902-5909.
31. Huybrechts, M.; Cuypers, A.K.; Deckers, J.; Iven, V.; Vandionant, S.; Jozefczak, M.; Hendrix, S. Cadmium and plant development: An agony from seed to seed. *Int. J. Mol. Sci*., **2019**, 20, 3971.
32. Paesano, L.; Perotti, A.; Buschini, A.; Carubbi, C.; Marmiroli, M.; Maestri, E.; Iannotta, S.; Marmiroli, N. Markers for toxicity to HepG2 exposed to cadmium sulphide quantum dots; damage to mitochondria. *Toxicology*. **2016**, 374, 18-28.
33. Lee, B.H.; Henderson, D.A.; Zhu, J.K. The Arabidopsis cold-responsive transcriptome and its regulation by ICE1. *Plant Cell*. **2005**, 17, 3155-3175.
34. Connolly, E.L.; Guerinot, M.L. Iron stress in plants. *Genome Biology* **2002**, 3, 1–4.
35. López-Millán, A.F.; Duy, D.; Philippar, K. Chloroplast iron transport proteins – Function and impact on plant physiology. *Front. Plant Sci*., **2016**, 7, 178.
36. Woloszynska, M. Heteroplasmy and stoichiometric complexity of plant mitochondrial genomes - though this be madness, yet there's method in't. *J. Experimental Botany*, **2010**, 61(3), 657-671.

37. Ruotolo, R.; Maestri, E.; Pagano, L.; Marmiroli, M.; White, J.C.; Marmiroli, N. Plant response to metal-containing engineered nanomaterials: an omics-based perspective. *Environ. Sci. Technol*. **2018**, 52 (5), 2451−2467.

38. Ma, Y.; Zhang, P.; Zhang, Z.; He, X.; Li, Y.; Zhang, J.; Zheng, L.; Chu, S.; Yang, K.; Zhao, Y.; Chai, Z. Origin of the different phytotoxicity and biotransformation of cerium and lanthanum oxide nanoparticles in cucumber. *Nanotoxicology* **2015**, 9 (2), 262−270.

39. Corral-Diaz, B.; Peralta-Videa, J.R.; Alvarez-Parrilla, E.; Rodrigo-García, J.; Morales, M.I.; Osuna-Avila, P.; Niu, G.; Hernandez-Viezcas, J.A.; Gardea-Torresdey, J.L. Cerium oxide nanoparticles alter the antioxidant capacity but do not impact tuber ionome in *Raphanus sativus* (L.). *Plant Physiol. Biochem.* **2014**, 84, 277-285.

40. Eriksson, P.; Tal, A.A.; Skallberg, A.; Brommesson, C.; Hu, Z.; Boyd, R.D.; Olovsson, W.; Fairley, N.; Abrikosov, I.A.; Zhang, X.; Uvdal, K. Cerium oxide nanoparticles with antioxidant capabilities and gadolinium integration for MRI contrast enhancement. *Sci. Rep*. **2018**, 8, 6999.

41. Iannone, M.F.; Groppa, M.D.; de Sousa, M.E.; van Raap, M.B.F.; Benavides, M.P. Impact of magnetite iron oxide nanoparticles on wheat (*Triticum aestivum* L.) development: evaluation of oxidative damage. *Environ. Exp. Bot*., **2016**, 131, 77-88.

42. Libralato, G.; Costa Devoti, A.; Zanella, M.; Sabbioni, E.; Mičetić, I.; Manodori, L.; Pigozzo, A.; Manenti, S.; Groppi, F.; Ghirardini, A.V. Phytotoxicity of ionic, micro- and nano-sized iron in three plant species. *Ecotoxicology and Environmental Safety*, **2016**, 123, 81-88.

43. Gallo, V.; Zappettini, A.; Villani, M.; Marmiroli, N.; Marmiroli, M. Comparative Analysis of Proteins Regulated during Cadmium Sulfide Quantum Dots Response in Arabidopsis thaliana Wild Type and Tolerant Mutants. *Nanomaterials* **2021**, 11, 615.

44. Jacoby, R.P.; Li, L.; Huang, S.; Lee, C.P.; Millar, A.H.; Taylor, N.L. Mitochondrial Composition, Function and Stress Response in Plants. *J. Integr. Plant Biol.*, **2012**, 54, 887–906.

45. Kazan, K.; Kalaipandian, S. Ferroptosis: Yet another way to die. *Trends in Plant Science*, **2019**, 24, 479-481.

46. Gómez, I.; Huovinen, P. Morpho-functionality of Carbon Metabolism in Seaweeds. In *Seaweed Biology. Novel Insights into Ecophysiology, Ecology and Utilization.* Ecological Studies 219; Wiencke, C.; Bischof, K. Eds; Springer, Berlin Heidelberg, 2012; pp. 25-46.

47. Chirino Miranda, E.; Ruiz-Yanetti, S.; Vilagrosa, A.; Mera, X.; Espinoza, M.; Lozano, P. Morpho-functional traits and plant response to drought conditions in seedlings of six native species of Ecuadorian Ecosystems. *Flora*. **2017**, 233, 58-67.

48. Krupinska, K.; Blanco, N.E.; Oetke, S.; Zottini, M. Genome communication in plants mediated by organelle–nucleus-located proteins. *Phil. Trans. R. Soc. B*. **2020**, 375, 20190397.

49. Bendich, A.J. Why do chloroplasts and mitochondria contain so many copies of their genome? Bioessays **1987**, 6, 279–282.

50. Bendich, A.J. DNA abandonment and the mechanisms of uniparental inheritance of mitochondria and chloroplasts. Chromosome Res. **2013**, 21, 287–296.

51. Shao, MR.; Kumar Kenchanmane Raju, S.; Laurie, J.D.; Sanchez, R.; Mackenzie, S.A. Stress-responsive pathways and small RNA changes distinguish variable developmental phenotypes caused by MSH1 loss. *BMC Plant Biol*. **2017**, 17, 47.

52. Carrie, C.; Small, I. A re-evaluation of dual-targeting of proteins to mitochondria and chloroplasts. *Biochim. Biophys. Acta* **2013**, 1833, 253–259.

53. Fulton, T.M.; Chunzoongse, J.; Tanksley, S.D. Microprep protocol for extraction of DNA from tomato and other herbaceous plants. *Plant Molecular Biology* **1995**, 13, 207-209.

54. Ni, Z.; Kim, E.D.; Chen, Z.J. Chlorophyll and starch assays. *Protoc. Exch*. **2009**, 19.

55. Porter, D.R.; Nguyen, H.T.; Burke, J. Quantifying acquired thermal tolerance in winter wheat. *Crop Sci*. 1**994**, 34, 1686-1689.

Figure captions

Figure 1. Target gene copy number variations on ptDNA and mtDNA. Schematic representation of *A. thaliana* ptDNA and mtDNA and relative position of the target genes taken into account (a, b). LSC: long single copy region; SSC: short single copy region; IRA, IRB: inverted repeated regions. Target genes were chosen so as to cover the entire ptDNA and mtDNA. Details related to the target genes are reported in the Supporting Information (SI). Distances were calculated on the basis of the NCBI reference sequences: chloroplast (AP000423.1), mitochondrion (NC_037304.1).

Heatmaps representing the chloroplast (c) and mitochondrial (d) relative target gene abundance during treatment with CdS QDs or $CdSO_4$, at different times of exposure and concentrations (Table 2). Data, normalized on the untreated control (T0 NT), showed a non-uniform target gene abundance across the entire ptDNA and mtDNA structures.

Relative target gene abundance of chloroplast (e) and mitochondrial (f) target genes taken into account during treatments with different ENMs and relative metal salts (Table 2). Data, normalized on the control untreated, highlighted the different ranges of similarity in the response (measured as relative target gene abundance) between the treatments with ENMs and relative metal ion counterparts. Numerical data are reported in Table S1.

Figure 2. Chord diagram graphical comparison between the relative gene abundance under treatment with ENM or relative metal salts in the chloroplast (a) and mitochondrion (b). Ribbons show the overlap between over- and under-abundant genes in term of copy number, normalized on the untreated control in the different treatments performed.

Figure 3. Heatmaps representing the physiological parameters measured: fresh biomass (mg);

photosynthetic pigments (chlorophyll *a*, chlorophyll *b*, and carotenoids absorbance) and cellular respiration (formazan absorbance). Data are reported in shades from lilac (higher values) to light blue (lower values). Data and statistics are reported in Tables S3-S5.

Figure 4. Principal Component Analysis (PCA) related to the effects on the chloroplast (a) and mitochondrion (b). For the chloroplast, parameters taken into account are the relative target gene copy number (ptDNA response), photosynthetic activity and biomass; for mitochondrion, the relative target gene copy number (mtDNA response), cellular respiration and biomass. The first component, representing 51.59% and 63.15% of the total variance for chloroplast and mitochondrion, respectively, is related to differential effects between the ENMs and their metal ion counterparts, as supported by biomass indices and DNA analyses.

Figure 5. Representation of mechanisms involved in the organellar DNA replication in response to oxidative stress due to ENMs exposure, with particular regard to CdS QDs. Molecular integrity can change drastically as a consequence of inhibition of respiration and photosynthesis, as well as from activation of photorespiration and ROS production. Abandonment of unrepaired organellar DNA molecules and replication of smaller DNA fragments have the role of blocking lesion transmission and modulating the availability of several gene functions.

Figure 6. ENMs characterization by transmission electron microscopy (TEM): (a) CeO_2 NPs, (b) Fe_2O_3 NPs, (c) Fe_3O_4 NPs, (d) ZnS QDs, (e) CdS QDs. Additional characterization data are reported in Table 1 and in the Supporting Information (SI).

Tables

Table 1. ENMs characterization related to aggregate average particle size (*dh*), zeta-potential (ζ), and dissolution after 20 days (in ddH_2O).

ENM	size (nm)	purity (%)	(ζ) Z-potential (mV)	(*dh*) hydrodynamic range (nm)	%metal	%dissolution
CeO_2 NPs	<25	99.99	+ 42.5	243.9	81.3	1
Fe_2O_3 NPs	<15	99.9	+ 3.8	978	69.8	16
Fe_3O_4 NPs	<10	99.9	+ 44.2	271.6	72.4	13
ZnS QDs	<5	99.99	+ 61.6	1190	63.2	3
CdS QDs	<5	99.99	+ 15.8	178.7	78	2

Concentration utilized for dissolution experiments was 100 mg L^{-1} for all the ENMs standards. Additional information related to ENM characterization has been reported in the Supporting Information (SI).

Table 2. ENMs treatments exposure time and concentrations used in experiment 1(a) and experiment 2(b).

(**a**)

name	exposure time	treatment	concentration	metal content	metal in solution*
T0 NT	0 days	untreated	0 mg L^{-1}	0 mg L^{-1}	0 mg L^{-1}
T10 NT	10 days	untreated	0 mg L^{-1}	0 mg L^{-1}	0 mg L^{-1}
T10 QD 40	10 days	CdS QDs	40 mg L^{-1}	31.2 mg L^{-1}	0.62 mg L^{-1}
T10 QD 80	10 days	CdS QDs	80 mg L^{-1}	62.4 mg L^{-1}	1.24 mg L^{-1}
T10 QD 150	10 days	CdS QDs	150 mg L^{-1}	117 mg L^{-1}	2.34 mg L^{-1}
T10 QD 250	10 days	CdS QDs	250 mg L^{-1}	195 mg L^{-1}	3.90 mg L^{-1}
T10 Cd(II) 50	10 days	$CdSO_4 \cdot 7H_2O$	38.4 mg L^{-1}	12.8 mg L^{-1}	12.8 mg L^{-1}
T10 Cd(II) 100	10 days	$CdSO_4 \cdot 7H_2O$	76.9 mg L^{-1}	25.6 mg L^{-1}	25.6 mg L^{-1}
T20 NT	20 days	untreated	0 mg L^{-1}	0 mg L^{-1}	0 mg L^{-1}
T20 QD 40	20 days	CdS QDs	40 mg L^{-1}	31.2 mg L^{-1}	0.62 mg L^{-1}
T20 QD 80	20 days	CdS QDs	80 mg L^{-1}	62.4 mg L^{-1}	1.24 mg L^{-1}
T20 QD 150	20 days	CdS QDs	150 mg L^{-1}	117 mg L^{-1}	2.34 mg L^{-1}
T20 QD 250	20 days	CdS QDs	250 mg L^{-1}	195 mg L^{-1}	3.90 mg L^{-1}

T20 Cd(II) 50	20 days	$CdSO_4 \cdot 7H_2O$	38.4 mg L^{-1}	12.8 mg L^{-1}	12.8 mg L^{-1}
T20 Cd(II) 100	20 days	$CdSO_4 \cdot 7H_2O$	76.9 mg L^{-1}	25.6 mg L^{-1}	25.6 mg L^{-1}

(**b**)

name	**exposure time**	**treatment**	**concentration**	**metal content**	**metal in solution***
untreated	20 days	untreated	0 mg L^{-1}	0 mg L^{-1}	0 mg L^{-1}
CeO_2 NPs	20 days	CeO_2 NPs	500 mg L^{-1}	407 mg L^{-1}	4.07 mg L^{-1}
$CeCl_3$	20 days	$CeCl_3$	175 mg L^{-1}	99.3 mg L^{-1}	99.3 mg L^{-1}
Fe_2O_3 NPs	20 days	Fe_2O_3 NPs	500 mg L^{-1}	349.9 mg L^{-1}	55.98 mg L^{-1}
Fe_3O_4 NPs	20 days	Fe_3O_4 NPs	500 mg L^{-1}	361.4 mg L^{-1}	46.98 mg L^{-1}
$FeCl_3$	20 days	$FeCl_3$	75 mg L^{-1}	25.4 mg L^{-1}	25.4 mg L^{-1}
ZnS QDs	20 days	ZnS QDs	500 mg L^{-1}	334 mg L^{-1}	6.64 mg L^{-1}
$ZnSO_4$	20 days	$ZnSO_4$	175 mg L^{-1}	70.8 mg L^{-1}	70.8 mg L^{-1}
CdS QDs	20 days	CdS QDs	80 mg L^{-1}	62.4 mg L^{-1}	1.24 mg L^{-1}
$CdSO_4$	20 days	$CdSO_4 \cdot 7H_2O$	76.9 mg L^{-1}	25.6 mg L^{-1}	25.6 mg L^{-1}

After 10 days growth on unamended MS medium, plants were transferred on to MS medium amended with the desired amount of ENMs or metal salts, (*) expected metal released in ddH_2O calculated from ENMs dissolution studies (Table 1).

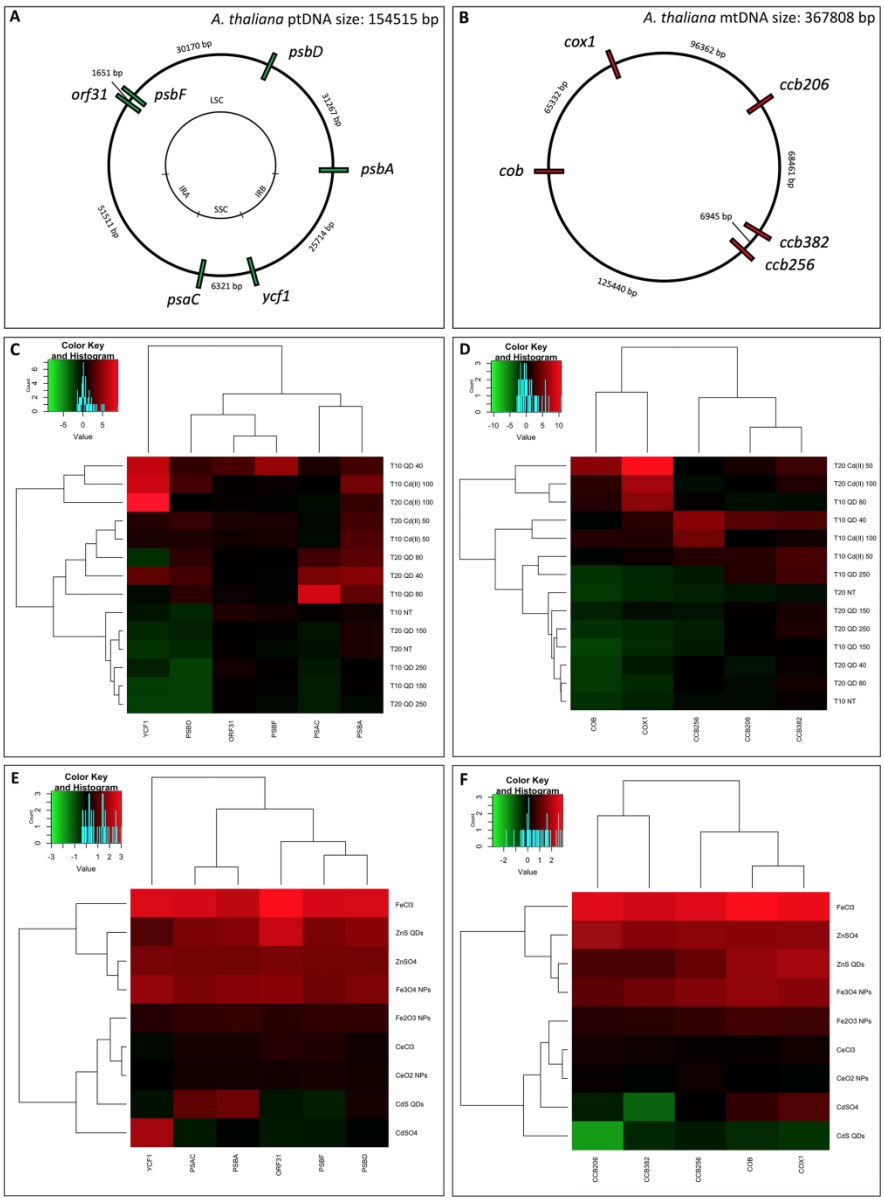

Figure 1. Target gene copy number variations on ptDNA and mtDNA. Schematic representation of A. thaliana ptDNA and mtDNA and relative position of the target genes taken into account (a, b). LSC: long single copy region; SSC: short single copy region; IRA, IRB: inverted repeated regions. Target genes were chosen so as to cover the entire ptDNA and mtDNA. Details related to the target genes are reported in the Supporting Information (SI). Distances were calculated on the basis of the NCBI reference sequences: chloroplast (AP000423.1), mitochondrion (NC_037304.1).

Heatmaps representing the chloroplast (c) and mitochondrial (d) relative target gene abundance during treatment with CdS QDs or CdSO4, at different times of exposure and concentrations (Table 2). Data, normalized on the untreated control (T0 NT), showed a non-uniform target gene abundance across the entire ptDNA and mtDNA structures.

Relative target gene abundance of chloroplast (e) and mitochondrial (f) target genes taken into account during treatments with different ENMs and relative metal salts (Table 2). Data, normalized on the control untreated, highlighted the different ranges of similarity in the response (measured as relative target gene abundance) between the treatments with ENMs and relative metal ion counterparts. Numerical data are

reported in Table S1

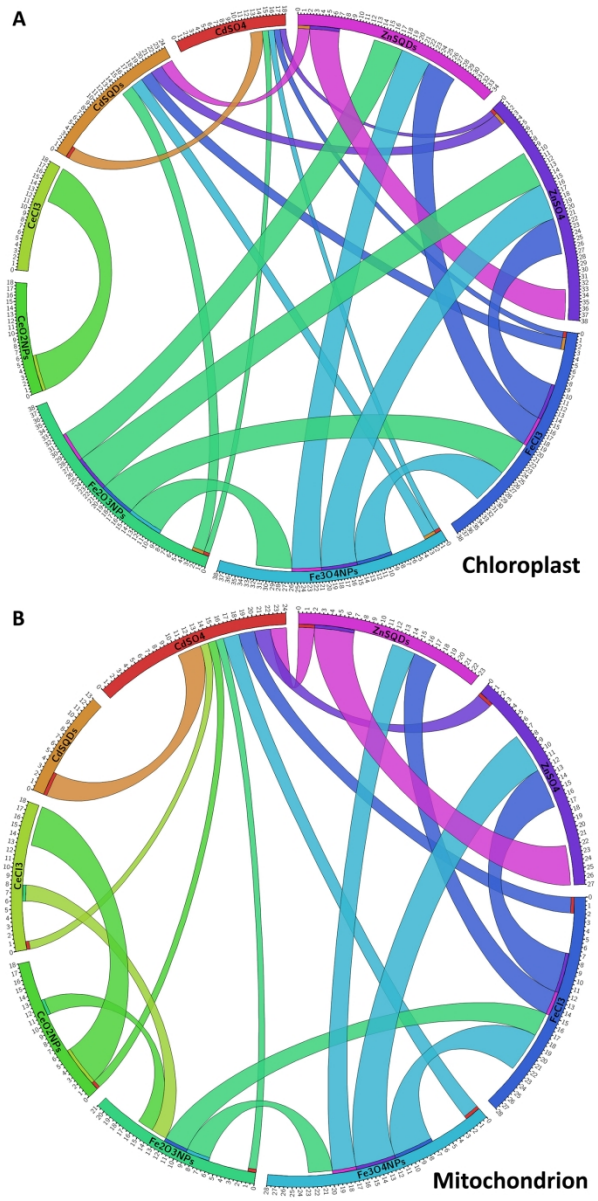

Figure 2. Chord diagram graphical comparison between the relative gene abundance under treatment with ENM or relative metal salts in the chloroplast (a) and mitochondrion (b). Ribbons show the overlap between over- and under-abundant genes in term of copy number, normalized on the untreated control in the different treatments performed.

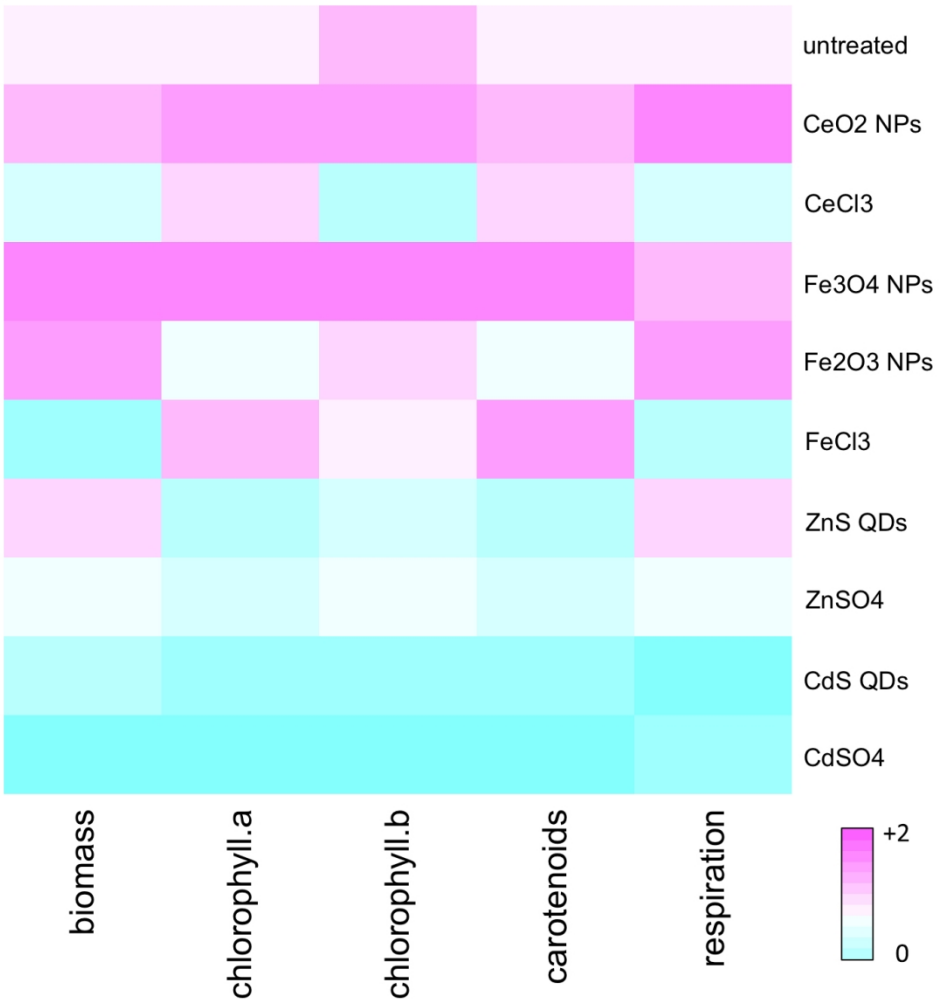

Figure 3. Heatmaps representing the physiological parameters measured: fresh biomass (mg); photosynthetic pigments (chlorophyll a, chlorophyll b, and carotenoids absorbance) and cellular respiration (formazan absorbance). Data are reported in shades from lilac (higher values) to light blue (lower values). Data and statistics are reported in Tables S3-S5

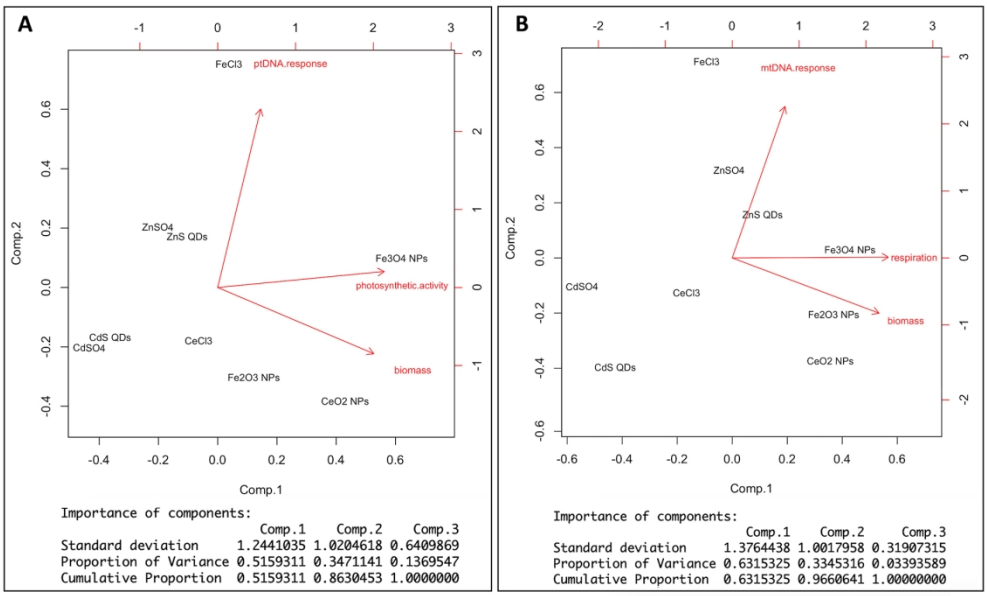

Figure 4. Principal Component Analysis (PCA) related to the effects on the chloroplast (a) and mitochondrion (b). For the chloroplast, parameters taken into account are the relative target gene copy number (ptDNA response), photosynthetic activity and biomass; for mitochondrion, the relative target gene copy number (mtDNA response), cellular respiration and biomass. The first component, representing 51.59% and 63.15% of the total variance for chloroplast and mitochondrion, respectively, is related to differential effects between the ENMs and their metal ion counterparts, as supported by biomass indices and DNA analyses.

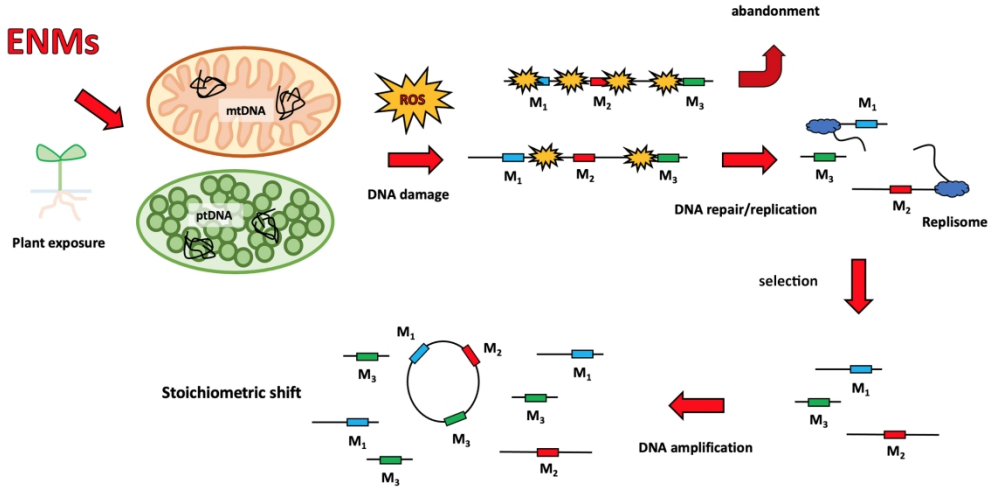

Figure 5. Representation of mechanisms involved in the organellar DNA replication in response to oxidative stress due to ENMs exposure, with particular regard to CdS QDs. Molecular integrity can change drastically as a consequence of inhibition of respiration and photosynthesis, as well as from activation of photorespiration and ROS production. Abandonment of unrepaired organellar DNA molecules and replication of smaller DNA fragments have the role of blocking lesion transmission and modulating the availability of several gene functions.

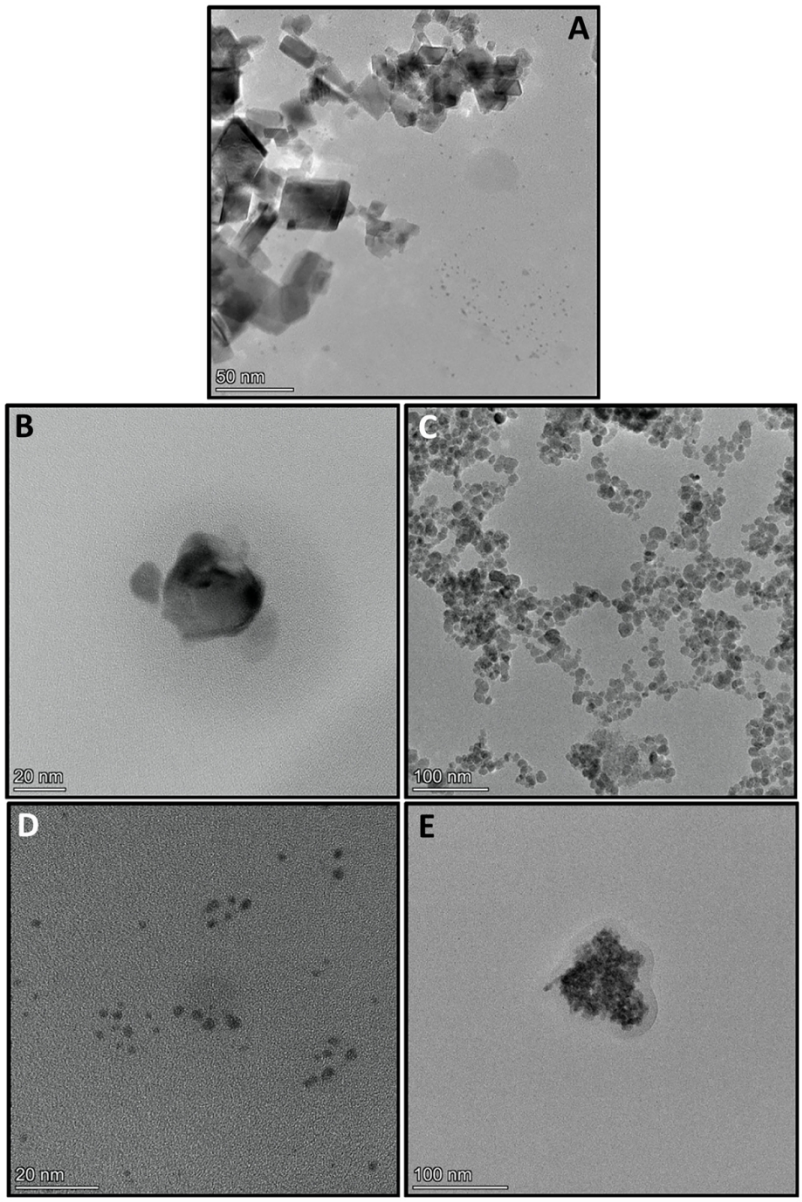

Figure 6. ENMs characterization by transmission electron microscopy (TEM): (a) CeO2 NPs, (b) Fe2O3 NPs, (c) Fe3O4 NPs, (d) ZnS QDs, (e) CdS QDs. Additional characterization data are reported in Table 1 and in the Supporting Information (SI).

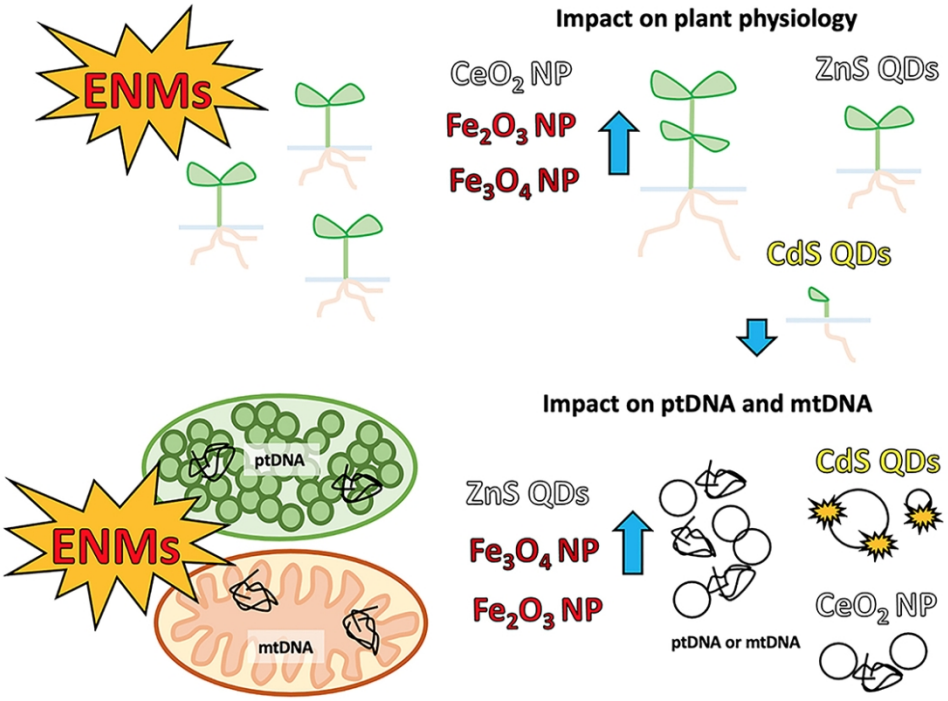
ENMs
Impact on plant physiology
CeO_2 NP
Fe_2O_3 NP
Fe_3O_4 NP
ZnS QDs
CdS QDs
ENMs
ptDNA
mtDNA
Impact on ptDNA and mtDNA
ZnS QDs
Fe_3O_4 NP
Fe_2O_3 NP
ptDNA or mtDNA
CdS QDs
CeO_2 NP

TOC